Solar Physics
DOI: 10.1007/•••••-•••-•••-••••-•

A Catalog of Bipolar Active Regions Violating the Hale Polarity Law, 1989 – 2018

Anastasiya Zhukova[1] · **Anna Khlystova**[2] · **Valentina Abramenko**[1] · **Dmitry Sokoloff**[3,4,5]

© Springer ••••

Abstract There is no list of bipolar active regions (ARs) with reverse polarity (anti-Hale regions), although statistical investigations of such ARs (bearing the imprint of deep subphotospheric processes) are important for understanding solar-cycle mechanisms. We studied 8606 ARs from 1 January 1989 to 31 December 2018 to detect anti-Hale regions and to compile a catalog. The *Solar and Heliospheric Observatory* (SOHO) and the *Solar Dynamics Observatory* (SDO) data, as well as the Debrecen Photoheliographic Data, the Mount Wilson Observatory catalog and drawings, and the USAF/NOAA Solar Region Summary were used. Complex, ambiguous cases related to anti-Hale region identification were analyzed. Two basic and four additional criteria to identify an AR as an anti-Hale region were formulated. The basic criteria assume that: i) dominating features of an AR have to form a bipole of reverse polarity with sunspots/pores

✉ A.V. Zhukova
anastasiya.v.zhukova@gmail.com

A.I. Khlystova
hlystova@iszf.irk.ru

V.I. Abramenko
vabramenko@gmail.com

D.D. Sokoloff
sokoloff.dd@gmail.com

[1] Crimean Astrophysical Observatory of Russian Academy of Sciences, Nauchny 298409, Bakhchisaray, Republic of Crimea

[2] Institute of Solar-Terrestrial Physics of Siberian Branch of Russian Academy of Sciences, Lermontov st., 126a, Irkutsk 664033, Russia

[3] Department of Physics, Lomonosov Moscow State University, Faculty of Physics, Leninskie Gory, 1-2, Moscow 119992, Russia

[4] Moscow Center of Fundamental and Applied Mathematics, Moscow 119991, Russia

[5] IZMIRAN, Kaluzhskoe shosse, 4, Troitsk, Moscow, 142191, Russia

arXiv:2010.14413v1 [astro-ph.SR] 27 Oct 2020

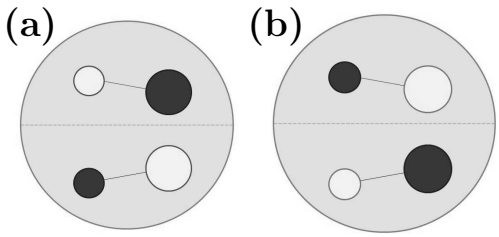


Figure 1. Regular (with the leading sunspot obeying Hale's polarity law) bipolar ARs in even (a) and odd (b) cycles. Sunspots with negative (positive) polarity are shown as black (white). The polarity of sunspots of anti-Hale regions is opposite.

of both polarities being present; ii) magnetic connections between the opposite polarities has to be observed. A catalog of anti-Hale regions (275 ARs) is compiled. The catalog contains: NOAA number, date of the greatest total area of sunspots, coordinates, and corrected sunspot area for this date. The tilt and the most complex achieved Mount Wilson magnetic class are also provided. The percentage of anti-Hale groups meeting the proposed criteria is ≈3.0 % from all studied ARs, which is close to early estimations by authors who had examined each AR individually: ≈2.4 % by Hale and Nicholson (*Astrophys. J.* **62**, 270, 1925) and ≈3.1 % by Richardson (*Astrophys. J.* **107**, 78, 1948). The enchancement of the anti-Hale percentage in later research might be related to: i) increasing sensitivity of instruments (considering smaller and smaller bipoles); ii) the ambiguities in the anti-Hale region identification. The catalog is available as the Electronic Supplementary Material and at the CrAO website (sun.crao.ru/databases/catalog-anti-hale/).

Keywords: Active Regions, Structure; Solar Cycle, Observations; Sunspots, Statistics

1. Introduction

The majority of active regions (ARs) obey the empirical rules for sunspot groups (Hale *et al.*, 1919): Hale's polarity law, Joy's law, etc. (regular ARs). The pioneering models of the magnetic cycle (Parker, 1955; Babcock, 1961; Leighton, 1964), as well as the global mean-field dynamo theory (see, e.g., Moffatt, 1978; Krause and Rädler, 1980), explain well the existance of the regular ARs. However, ARs violating these empirical rules also occur. According to Hale's law during an even (odd) sunspot cycle, the leading sunspot of a bipolar AR has negative (positive) polarity in the northern hemisphere and the situation is reversed in the southern hemisphere. A sketch of regular ARs of even (odd) cycles is presented as Figure 1. In this article, we deal with bipole sunspot groups with the reverse polarity (anti-Hale regions). We do not consider here other types of irregularities.

Anti-Hale ARs bear the imprint of deep subphotospheric processes. So, statistical studies of these ARs may shed light on our understanding of solar magnetic-field evolution and solar-cycle mechanisms. For instance, Sokoloff, Khlystova, and Abramenko (2015) found that a contribution of small-scale fluctuation dynamo in the interplay with the global dynamo is more pronounced at solar-cycle

minimum. The authors came to this conclusion based on their probabilistic model and the revealed enhancement of the relative number of anti-Hale regions during solar minimum. Note that the presence of magnetic-field fluctuations on smaller (as compared to the mean-field) scales was earlier predicted by both the turbulent dynamo theory (e.g. Kraichnan and Nagarajan, 1967; Kazantsev, 1968; Zeldovich, Ruzmaikin, and Sokoloff, 1990; Brandenburg and Subramanian, 2005) and direct numerical simulations (e.g. Blackman and Field, 2002; Rädler, Kleeorin, and Rogachevskii, 2003; Sur, Brandenburg, and Subramanian, 2008; Brandenburg, Sokoloff, and Subramanian, 2012). The decay of anti-Hale ARs can explain the weakening of the polar magnetic field: the transport of remnants of the following parts of anti-Hale regions to the poles causes the decrease of the polar field (Mordvinov and Kitchatinov, 2019). Numerical simulations by Hazra, Choudhuri, and Miesch (2017) show that the high-latitude anti-Hale ARs in the middle phase of a cycle must contribute to weakening of the polar field more than the rest of anti-Hale groups. Jiang, Cameron, and Schüssler (2015) also found that the magnetic-flux advection through the Equator due to decay of anti-Hale ARs causes the weakening of the process of the polar-field recovery. Determination of the magnetic twist and writhe for several ARs attributed as anti-Hale regions allowed López Fuentes *et al.* (2000, 2003) to estimate the degree of influence of various mechanisms (kink-instability, effect of the Coriolis force, etc.) on the deformation of flux-tubes. Thus, the observational data on the statistics and properties of anti-Hale groups is in high demand in the solar physics community.

Unfortunately, there is no reliable database of anti-Hale regions. Although many catalogs provide information on the polarity of leading and following parts of ARs and use this information (for example, to measure the tilt of the sunspot-group axis), the catalogs do not provide these data explicitly. The Mount Wilson Observatory (MWO) catalog had been a main data source on the anti-Hale ARs for a long time. The catalog had been replenished irregularly since 1920. The data are available digitally since 1962. From 1989 to 2004 the ARs of reverse polarity are marked with the sign "+". According to many researchers who examined the catalog, some ARs in the catalog are marked with this sign erroneously. Thus, Hale and Nicholson (1925) viewed a lot of AR drawings to verify the magnetic class detected by MWO operators. Richardson (1948) reported checking each AR of reverse polarity from the MWO catalog based on the initial records. Errors in anti-Hale region identification in the MWO catalog were also revealed by Sokoloff, Khlystova, and Abramenko (2015).

The published estimation of the relative number of anti-Hale regions varies within a rather wide range: from a few percent to approximately (8 – 9)%. Hale and Nicholson (1925) found that <6 (2.4 on average) of all ARs are the reverse-polarity groups with simple bipolar magnetic configuration. Later the following results for this parameter were reported: 3.1 (Richardson, 1948), <5 (Smith and Howard, 1968), 1.8 (Vitinsky, 1986), 4 (Wang and Sheeley, 1989); 4.9 (Khlystova and Sokoloff, 2009, Sokoloff and Khlystova, 2010), 4 (Stenflo and Kosovichev, 2012), ≈8 (Li and Ulrich, 2012; McClintock, Norton, and Li, 2014; Li, 2018). Note that only part of these studies were performed on the basis of the MWO catalog. Many authors used their own databases. McClintock, Norton, and Li

(2014) suggested that the inhomogeneity of the data used might be the reason for such a discrepancy in the results of various authors. The size of included ARs is one of the main reasons for discrepancy, because small sunspot groups are prone to violate the Hale's polarity law more frequently (Richardson, 1948; Howard, 1989; Stenflo and Kosovichev, 2012). Only ≈60 % of ephemeral regions obey this law (Hagenaar, 2001). Moreover, the smallest quiet-Sun bipoles are randomly oriented (Tlatov, Vasil'eva, and Pevtsov, 2010).

Errors in the identification of anti-Hale regions also occure. For example, there is an obvious difference in numbers and coordinates of anti-Hale ARs on the time–latitude diagrams reported by Richardson (1948) and by Vitinsky (1986) in spite of the fact that the authors used the same database. The known reasons for anti-Hale region misidentification are: i) erroneous detection of ARs boundaries (Sokoloff, Khlystova, and Abramenko, 2015); ii) the wrong distribution of ARs between cycles during the transition from one solar cycle to anoter; iii) the misalignment between the magnetic and the heliographic Equators. The two latter reasons are discussed by McClintock, Norton, and Li (2014).

When compiling a database for further identification of anti-Hale regions, the type of the source data (magnetograms, drawings, etc.) is also important. Thus, Stenflo and Kosovichev (2012) reported about the objective difficulties in automatic detection of individual sunspot groups from full-disk magnetograms and extraction of single ARs. Besides, inaccuracies related to detection of weighted centers of polarities may also produce errors. Wang *et al.* (2015) revealed that white-light measurements generally underestimate the tilts (axial inclinations) of ARs, even when the leading- and the following-polarity sectors are identified correctly.

To summarize, studies of anti-Hale regions are essential for understanding the solar dynamo. So far, there is no reliable list of ARs with reverse polarity. We undertake a compilation of such a database starting from 1989 and covering the last two and a half solar cycles. We paid special attention to the analysis of mistakes and ambiguities in identification of anti-Hale ARs.

2. Data and Method

2.1. Data Sources

To examine ARs visually, we used the full-solar-disk daily data: magnetograms, continuum and extreme ultraviolet (EUV) images, sketches and drawings, as well as different images of the individual ARs. We also used available catalogs containing the information on the leading sunspot polarity of bipolar ARs and other necessary data. We used the following sources:

– the Michelson Doppler Imager (MDI: Scherrer *et al.*, 1995) and the Extreme Ultraviolet Imaging Telescope (EIT: Moses *et al.*, 1997) on board the Solar and Heliospheric Observatory (SOHO);

– the Helioseismic and Magnetic Imager (HMI: Scherrer *et al.*, 2012) and the Atmospheric Imaging Assembly (AIA: Lemen *et al.*, 2012) onboard the Solar Dynamic Observatory (SDO);

– the Debrecen Photoheliographic Data (DPD)
(Baranyi, Győri, and Ludmány, 2016) accessible from
fenyi.solarobs.csfk.mta.hu/DPD/;

– the websites www.helioviewer.org (Helioviewer), www.solarmonitor.org (Solar Monitor);

– the MWO drawings - which are available in the digital archive at
ftp://howard.astro.ucla.edu/pub/obs/drawings/;

– the MWO catalog accessible at the National Geophysical Data Center at
ftp://ftp.ngdc.noaa.gov/STP/SOLAR_DATA/SUNSPOT_REGIONS/
Mt_Wilson/;

– the Crimean Astrophysical Observatory (CrAO) catalog
(Abramenko, Zhukova, and Kutsenko, 2018; Zhukova, 2018) at
sun.crao.ru/databases/catalog-mmc-ars;

– the United States Air Force/National Oceanic and Atmospheric Administration Solar Region Summary (USAF/NOAA SRS) at
solarcyclescience.com/activeregions.html.

Note that at the biginning of our study we also used the Royal Observatory, Greenwich – USAF/NOAA Sunspot Data provided by the National Aeronautics and Space Administration (NASA). But these data are available only until October 2016 (solarscience.msfc.nasa.gov/greenwch.shtml), and later we restricted ourselves to the USAF/NOAA SRS database.

2.2. Ambiguities in Anti-Hale Region Identification

We encountered the following ambiguities in anti-Hale AR identification.

i) During solar-cycle minima the high-latitude sunspot groups (new-cycle precursors) might be erroneously accepted as reverse-polarity ARs. The periods of this ambiguity are 1996 and 2008 (the cycle minima). To determine what cycle a suspicious high-latitude group belongs to, we used a technique suggested by McClintock, Norton, and Li (2014). The boundaries between cycles in North and South hemispheres were defined as:

$$60 \times ylat = \pm(xdate - xint), \tag{1}$$

where $ylat$ is latitude, $xdate$ is a function of a number of days from 1 January 1974, and $xint$ (a point of inter section at the Equator) was visually determined separately for the best fit for each cycle. The time–latitude diagram based on the USAF/NOAA SRS sunspot-group data is presented as Figure 2. Cycle boundaries for Solar Cycles 22/23 and 23/24 are plotted from McClintock, Norton, and Li (2014) data. We also plotted here the fit of the boundary between Solar Cycles 24 and 25. This boundary might be slightly changed with Solar Cycle 25 evolution.

ii) Detection of individual sunspot groups in large composite activity complexes represents a challenge. Stenflo and Kosovichev (2012) supposed that it does not seem feasible to make a program that can automatically and reliably identify *all* of the bipolar regions. Blocks and chains of ARs are typical for solar maxima. In that and some other cases sunspots/pores may be attributed with

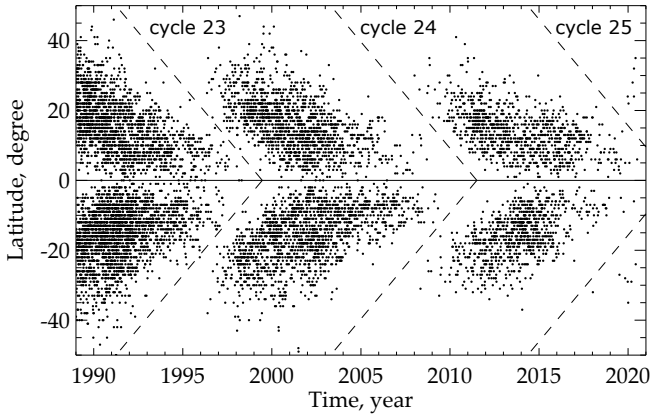


Figure 2. Time–latitude diagram of sunspot groups (by USAF/NOAA SRS data) with boundaries (dotted lines) between cycles plotted by McClintock, Norton, and Li (2014) technique.

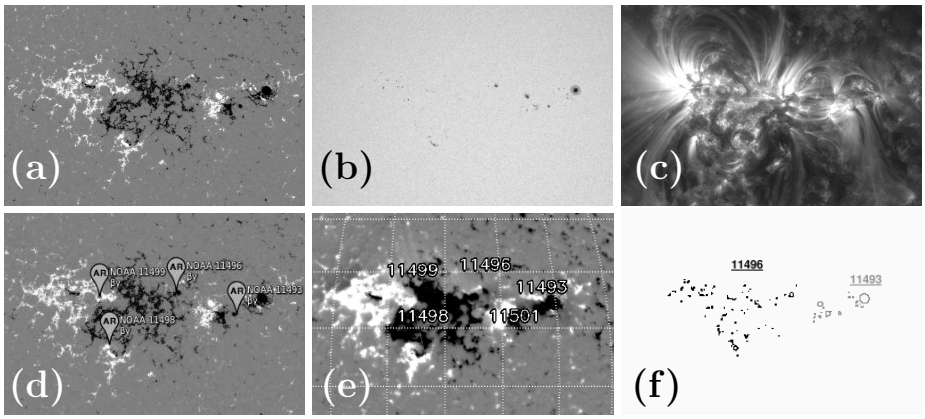


Figure 3. Composite activity complex observed on 06 June 2012 in the North hemisphere: HMI magnetogram (a), continuum (b), and AIA Fe IX/X 171 Å line (c) images. Helioviewer (d), Solar Monitor (e), and DPD (f) interpretations of AR detection as an illustration of the difference in AR-separation algorithms. There are no anti-Hale regions in this block of ARs.

equal probability to several adjacent groups. Differences in segmentation of a magnetic complex by various tools is illustrated in Figure 3. We assumed that there are no anti-Hale sub-regions in this particular case.

iii) Phenomena in ARs in the late decaying stage when the following spots of an AR have vanished or weakened:

a) Presence of opposite polarity small sunspots/pores to the West of an old leading sunspot. To illustrate, an example of a large decaying AR is shown in Figure 4. Magnetic connections between a large leading spot of positive polarity and fragmented pores of negative polarity to the East are evident and steady (panels c, f). Such magnetic loops is the typical connection of the leading and the following parts of bipolar ARs. The absense of a magnetic connection between the large leading spot and a negative polarity pore to the South-West does not allow us to identify this couple of sunspots as a single AR with reverse polarity.

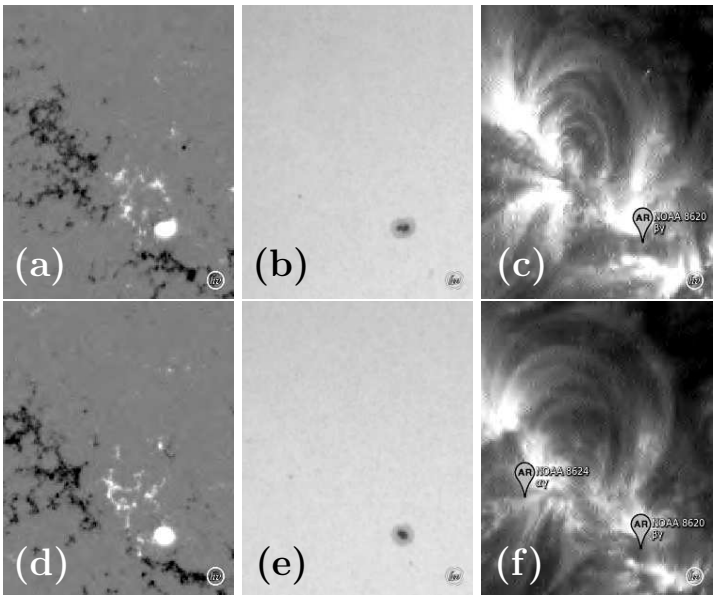


Figure 4. Sunspot group in the North hemisphere assigned by Helioviewer as a single AR 8620 on 06 July 1999: HMI magnetogram (a), continuum (b), and AIA Fe IX/X 171 Å line (c) images; the same images of this sunspot group on 07 July (d, e, f): two separate ARs (NOAA 8620 and 8624) are assigned. A part of the mafgnetic structure assigned as NOAA 8620 on panel (f) is not a true anti-Hale AR because there is no magnetic connection between sunspots.

Note, however, that this couple of sunspots is assigned by Helioviewer as an individual AR NOAA 8620 on 07, 09 July 1999 and further; the following part of the initial sunspot group is extracted by Helioviewer as AR NOAA 8624. Such situation is typical for an AR with complex magnetic configuration (classified "γ" in the Mount Wilson class).

Moving magnetic features might also cause emerging of pores on moat–cell boundaries (Ryutova, 2018). The combination of the old leading spot and opposite-polarity small spot/pore to the West of it may be misidentified as a separate sunspot group violating Hale's polarity law (Figure 5), especially by automatic algorithms.

b) Presence of opposite polarity pores all around the old sunspot. In cases when the flux (area) weighted center of scattered pores is located to the West of the old spot, the AR also might be erroneously identified as an anti-Hale region.

We did not include the above mentioned cases in the compiled catalog.

iv) Tilt instability of emerging ARs. The tilt is known to be unstable during several days after the emergence onset (see, e.g., van Driel-Gesztelyi and Green, 2015; Schunker *et al.*, 2020) and may change the orientation importantly. One cannot determine the leading/following sunspot position and polarity unambiguously while the tilt is not stabilized. So, it is a challenge to establish a reverse polarity for the groups arising in the close proximity to the western limb, as well as for small short-lived ARs. We discarded ARs emerging near the western limb and observed only for one or two days. All short-lived ARs (having spots/pores

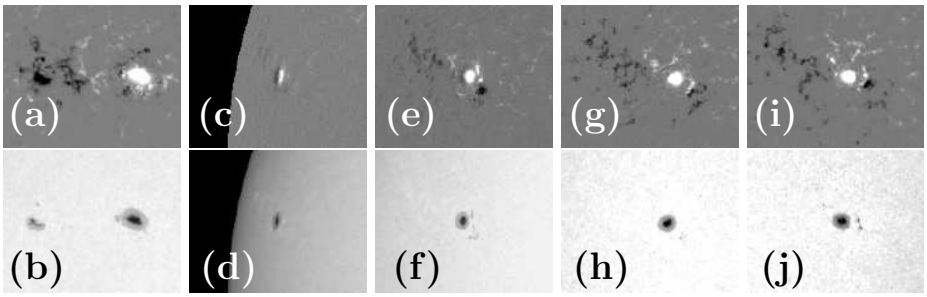


Figure 5. Recurrent AR NOAA 10634 (the North hemisphere) on 19 June 2004 (a,b) and its evolution as AR NOAA 10644 in the next rotation on 11 July 2004 (c,d), 13 (e,f), 15 (g,h), 17 (i,j) illustrated by MDI magnetograms (upper panel) and continuum images (lower panel). Spots/pores in the following polarity of AR NOAA 10644 are absent; the decay of the long-living leading sunspot is accompanied by the formation of small spots/pores on the moat–cell boundaries. The combination of this with the old leading sunspot might be misidentified as an anti-Hale AR.

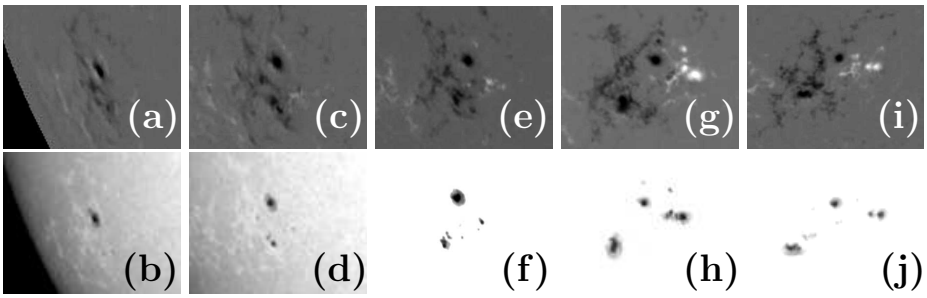


Figure 6. Evolution of AR NOAA 9264 (the South hemisphere) illustrated by MDI magnetograms (upper row) and continuum images (bottom row) on 11 December 2000 (a,b), 12 (c,d), 13 (e,f), 15 (g,h), 17 (i,j). A new reverse-polarity bipole emerged near the old unipolar spot.

of both polarities for less than three days) and ARs with tilt uncertainties were indicated with special marks: "S" and "T", respectively (see Section 3.2).

v) Emergence of a new reverse-polarity bipole close to a pre-existing unipolar sunspot. Sometimes such new bipoles have an individual NOAA number, e.g. ARs NOAA 7062 close to 7056, and sometimes they do not. We extracted the new anti-Hale region from the whole activity complex (in the latter case, under the hosting NOAA number). In the catalog, they are marked by "X". A typical example is shown in Figure 6. This procedure was applied only for emerging anti-Hale regions that survived longer than three days. Sunspot areas for extracted ARs were calculated by using a technique described in Section 3.2.

vi) ARs changing their properties during the displacement across the disk. Some ARs, when passing across the disk, show anti-Hale properties for only a part of time. It may be due to emergence of a new magnetic flux in the vicinity. In other cases, a bipolar sunspot group with reverse-polarity remains after the decay of a multipolar AR. If the reverse-polarity property is observed longer than three days, we noted this region with a special mark "P".

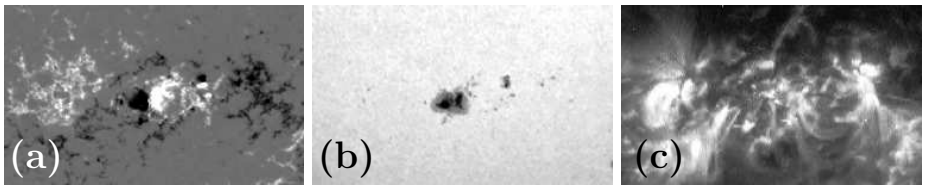


Figure 7. Complex AR NOAA 9591 including magnetic "δ-configuration" sunspot observed on 28 August 2001 in the South hemisphere: MDI magnetogram (a), continuum (b), and AIA Fe IX/X 171 Å line (c) images. The "δ-sunspot" of reverse polarity was extracted and considered in the compiled catalog.

vii) ARs with the main spots of both polarities near the Equator. McClintock, Norton, and Li (2014) argue that equatorial location of sunspot groups is related to a misalignment of the magnetic and heliographic Equators. They suppose that ARs such as NOAA 11987, for example, pertain to the magnetic system of the North hemisphere despite the fact that the leading spot is located a bit below the Equator. The authors explain such phenomena by the different degree of activity of the North and South hemispheres. Considering these reasons, we included into the catalog only those near-Equator ARs where the area-weighted center and the midpoint between the main spots of both polarities belong to the same hemisphere. They are marked with a letter "E".

viii) ARs with "δ-configuration". This class of ARs was introduced for sunspot groups with closely spaced opposite-polarity umbrae located in the common penumbra and added to the initial Mount Wilson magnetic classification by Künzel (1965). A sample of AR NOAA 9591 including "δ-sunspot" is presented as Figure 7. Individual "δ-structures" with reverse polarity were included in our database with the mark "D". "δ-spots" amidst the spread out background magnetic complex (see Figure 7) were extracted and considered only in the cases when such a "δ-structure" was the strongest feature in the entire complex. In case the extracted "δ-structure" displays the reverse polarity, we indicated it with the mark "W". There are only seven such events in the compiled catalog.

ix) Multipolar ARs. A sample of such AR (NOAA 10069) is shown in Figure 8: a number of equivalent-by-size sunspots of both polarities are spread around without forming any single bipole. Sometimes the most western spots may have the wrong polarity according to the Hale's polarity law, see Figure 8. In spite of this attribute, we decided not to count multipolar ARs in out dataset. Examples of multipolar ARs are: NOAA 6562, 6624, 10501, 10786, and 12673.

x) The polarity of sunspots may be reversed due to the projection effect. Of course, such cases were not counted.

2.3. Shortcomings in the Existing Data Sources

We also encountered issues related to data sources.

i) Flaws of the MWO data:

a) Lack of records (e.g. ARs NOAA 7926, 9858, and 10268) because of different reasons, including weather conditions (e.g. ARs NOAA 6255, 7430,7872, and 8963).

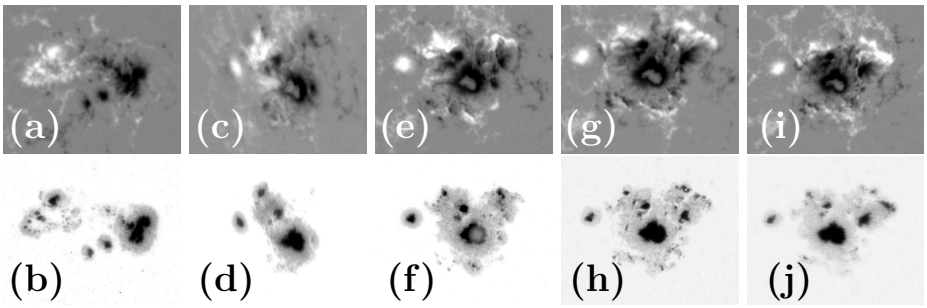


Figure 8. Recurrent AR NOAA 10036 (the South hemisphere) on 22 July 2002 (a,b) and its evolution as AR NOAA 10069 in the next rotation on 14 August 2002 (c,d), 16 (e,f), 17 (g,h), 18 (i,j) illustrated by MDI magnetograms (upper row), DPD (Gyula Observing Station and Debrecen Heliophysical Observatory) continuum images (bottom row). The old leading sunspot is surrounded by opposite-polarity sunspots since 16 August; some of them are located at the western part of the AR. This one and similar multipolar ARs were not included in the catalog.

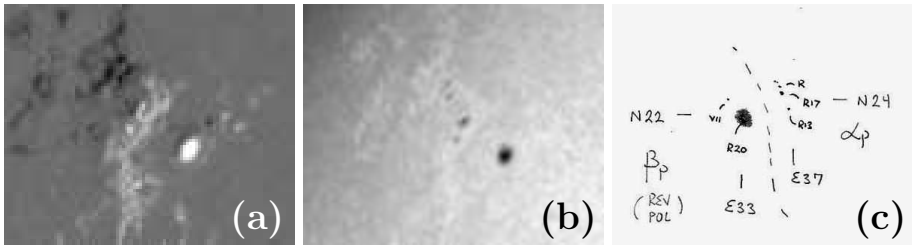


Figure 9. AR NOAA 9294 observed on 04 January 2001 in the North hemisphere: MDI magnetogram (a) and continuum image (b). (c) an erroneous identification of the group as a group of reverse polarity on the MWO drawing.

b) Wrong determination of the magnetic-field polarity (all sunspots/pores of a bipolar AR are marked as the same polarity features, e.g. ARs NOAA 8023, 9470, and 9699). Wang *et al.* (2015) also reports that such cases are multiple among ARs with the polar separation less than 2.5 degrees.

c) Erroneous usage or lack of the mark "REV. POL." (reversed polarity) on MWO drawings. A sample of an AR with proper polarity of the leading sunspot, but wrongly marked as "REV. POL." is presented in Figure 9. The magnetogram and the continuum image have the usual EW-orientation whereas the MWO drawing has the opposite orientation. The main spot R20 has a regular (for leading spots in Solar Cycle 23 in the North hemisphere) positive polarity, but the AR is marked as "REV. POL.". The opposite situation is observed in the MWO catalog for the anti-Hale ARs NOAA 5622, 7741, 7948, 8210, 9045, 9736, and 10638, which are not marked as reverse-polarity ARs.

d) Lack of AR NOAA number.

ii) Uncertainties in AR NOAA assignement in the DPD, the USAF/NOAA SRS databases, Solar Monitor, and Helioviewer:

a) After the decay of an AR, the same NOAA number was assigned to a new anti-Hale region that emerged at the same location (e.g. ARs NOAA 6241, 7324) or nearby (e.g. AR NOAA 7062);

b) Differences in outlining of boundaries (areas) of ARs in the USAF/NOAA SRS and the DPD databases. For example, according to the DPD, the anti-Hale AR NOAA 12310 is a single active region. But according to the USAF/NOAA SRS and Solar Monitor, this complex is fragmented into three different ARs (NOAA 12310, 12312, and 12313). Another example: AR NOAA 6203 is classified as a single group on the DPD sketch, and as two separate ARs (including the anti-Hale bipolar group MWO number 26212) on the MWO drawing.

ARs with such ambiguities in various databases were indicated with mark "N".

iii) Errors in calculations of sunspot-group areas. For instance, in the USAF/NOAA SRS database on 13 July 1994 AR NOAA 7746 has an extremely high value of the group area, which triply exceeds that reported for previous and following days. At the same time, the DPD data show a smooth change of this value.

To this end, to provide a database of anti-Hale regions without the aforementioned shortcomings, we examined anew all ARs from 1989 to 2018.

3. The Compiled Catalog

3.1. Anti-Hale Regions Selection Criteria

When elaborating our criteria of identification of anti-Hale regions, we were guided by original ideas by Hale and Nicholson (1925). We also assumed that the main spots of different polarities are footpoints of emerged magnetic loops in accordance with classic magnetic-cycle models (Babcock, 1961; Parker, 1955). Following this, we formulated two basic criteria for identification of an AR as an anti-Hale region.

i) Dominating features of an AR form a bipole of reverse polarity with sunspots or pores of both polarities being present.
ii) Magnetic connections between the opposite polarities are steady: magnetic loops (arcades) are visible at least in one of the EUV images day by day (in the cases when EUV data are available).

The remaining four additional criteria are proposed for certain ambiguous types of ARs.

iii) For small, short-lived (less than three days) sunspot groups. The tilt of an AR has to be stable (not rotating, not perpendicular to the Equator). The rotation of the tilt more than 20 degrees during the interval of observation was considered as a non-stable tilt. The area of an AR must be greater than 4 μHem and the corrected umbra area by the DPD must be non-zero (to exclude ambiguous pores: "transient" and "penumbrae without umbrae" features, see Lefevre and Clette 2014).
iv) For sunspot groups located on the Equator. Both the area-weighted center and the midpoint between the polarities of an AR have to be located in the same (the North or South) hemisphere.
v) For emerging bipolar groups appearing from a pre-existing AR. The extracted bipole has to exist at least three days.

vi) For "δ-structures" amidst the background magnetic complex. The extracted "δ-structure" has to form the strongest feature in the magnetic complex and does not have steady magnetic connections with other magnetic centers of the complex.

We did not consider any unipolar sunspots. We also did not consider multipolar ARs.

3.2. Anti-Hale Database and Special Marks

All detected anti-Hale ARs are listed in the database (see the Electronic Supplementary Material). Several lines from the catalog beginning, as well as the two last lines of the catalog are shown as Table 1. For each AR, the catalog includes three information blocks: i) the USAF/NOAA SRS data; ii) the DPD data; iii) our special marks. The first and second blocks each include the following parameters: the NOAA (or DPD) number; the date of the greatest corrected total area of sunspots in D M Y (day, month, year) format. For this date, we show: latitude (LAT), longitude (LON), the maximum value of the corrected total sunspots area (Area). Area values are provided in millionths of the solar hemisphere (μHem).

The most complex Mount Wilson magnetic class (Hale class) achieved by a given AR is also shown in the USAF/NOAA SRS data block. When the Mount Wilson magnetic class was not available, we assigned this class. For ARs that exhibit the anti-Hale behaviour only for a partial time during the evolution, we considered only the anti-Hale period to determine the Mount Wilson magnetic class.

The DPD block contains the tilt information for the ARs studied. Unfortunately, there is a lack of tilt data from 2014 to 2018 in the DPD database (except for some months in 2017). The sign "z" stands for missing data. The data on the recurrent ARs are provided in the catalog for each rotation separately.

We use the following special marks for particular types of ARs:

C – decaying (**C**ollapsing) ARs;

D – individual "δ-sunspots";

E – **E**quatorial ARs;

N – ARs with ambiguities in the **N**OAA numbers assignment and/or outlining of boundaries of sunspot groups in various databases;

P – an AR exhibits the anti-Hale property only **P**art time when passing across the disk;

R – ARs with **R**otation of the sunspot-group axis;

S – small **S**hort-lived ARs;

T – ARs with the **T**ilt close to 90°;

V – ARs which are not checked for the stability of magnetic connections (lack of EU**V** data);

W – "δ-sunspots" **W**ith surrounding sunspots/pores;

X – e**X**tracted ARs.

The extracted ARs were counted with the hosting AR NOAA numbers. Area values in such cases were determined as follows. For the DPD data block, the

Table 1. Catalog of the anti-Hale regions

	USAF/NOAA SRS								DPD							marks							
No.	NOAA	D	M	Y	LAT, [degr.]	LON, [degr.]	Area, [μHem]	Hale class	NOAA /DPD	D	M	Y	LAT, [degr.]	LON, [degr.]	Area, [μHem]	Tilt, [degr.]	1	2	3	4	5	6	7	AC
1	5409	23	03	1989	18.0	14.0	990	BGD	5409	22	03	1989	16.79	12.46	1334	-26.93				P		V		1.00
2	5414	24	03	1989	-18.0	49.0	150	B	5414	21	03	1989	-18.01	20.65	238	26.55						V		1.00
3	5441	10	04	1989	36.0	-15.0	330	BD	5441	08	04	1989	35.03	-29.55	506	-24.66						V		1.00
4	5455	14	04	1989	19.0	-58.0	20	B	5455	15	04	1989	24.93	-31.74	6	-17.10	S					V		1.00
5	5470	05	05	1989	28.0	-17.0	520	BGD	5470	04	05	1989	29.44	-16.97	775	15.82						V		1.00
6	5504	24	05	1989	22.0	-9.0	20	B	5504	23	05	1989	22.27	-7.07	17	21.93	S					V		1.00
7	5548	17	06	1989	-22.0	58.0	10	A	5548	16	06	1989	-21.55	57.96	5	-47.77	S	T				V		1.00
8	5600	22	07	1989	-18.0	-35.0	10	B	5600	22	07	1989	-19.42	-27.01	37	zzzzz				X		V		0.52
9	5622	09	08	1989	-26.0	44.0	280	B	5622	08	08	1989	-26.07	42.26	444	-13.28				P		V		1.00
10	5648	17	08	1989	7.0	14.0	10	B	5648	17	08	1989	6.80	29.83	9	-5.91	S					NV		1.00
11	5656	23	08	1989	26.0	-32.0	10	B	5656	23	08	1989	25.46	-18.97	12	0.50	S					V		1.00
12	5703	22	09	1989	-23.0	-45.0	60	B	5703	21	09	1989	-22.14	-44.66	72	19.27	C			P		V		1.00
13	5729	06	10	1989	-28.0	-61.0	50	B	5729	08	10	1989	-28.25	-24.43	49	-0.99						V		1.00
14	5747	19	10	1989	-27.0	-22.0	1160	BD	5747	19	10	1989	-26.72	-12.04	1354	-38.64		D	T	R	P	V		1.00
...																								
274	12703	31	03	2018	-8.0	-60.0	10	A	12703	30	03	2018	-9.17	-71.68	24	zzzzz	C							1.00
275	12720	26	08	2018	8.0	39.0	100	B	zzzzz	zz	zz	zzzz	zzzzzz	zzzzzz	zzzz	zzzzz								1.00

area of each extracted bipole at the evolutionary maximum was found as a total of composing sunspots. For the USAF/NOAA SRS data block (the individual sunspot-area data are absent), we used a different method. From the DPD data, we determined the moment of the maximal evolution for a given extracted anti-Hale region. Then, an auxiliary coefficient was found (also from the DPD data) as a ratio of the corrected total sunspot area of the extracted anti-Hale region

to the corrected total sunspot area of the entire hosting group. This coefficient was applied to the area value of the hosting AR from the USAF/NOAA SRS database (at the same date) to calculate the anti-Hale region area. The auxiliary coefficient marked as "AC" is shown in the last column of the catalog.

Areas of ARs with shortcomings in areal data (see Section 2.3) were calculated by special procedure. For example, only the areas of relevant sunspots were counted for AR NOAA 12310 for the DPD data block.

4. Estimations of the Relative Number of Anti-Hale Regions

In total, we studied 8606 ARs of Solar Cycles 22, 23, and 24. 275 sunspot groups were identified as anti-Hale regions and included in the catalog. We found the anti-Hale percentage as ≈3.2, and ≈3.0 in the case of excluding short-lived ARs with unsteady tilt. This estimation is close to previous earliest results by Hale and Nicholson (1925), ≈2.4, and by Richardson (1948), ≈3.1.

However, as we show in the Introduction, the recent studies of anti-Hale regions provide a higher percentage of 4 – 8. Possible reasons for this are discussed below.

We found that small short-lived groups (96 ARs) comprise about a one third of our set of anti-Hale regions. Exclusion of these ARs changes the anti-Hale percentage significantly (down to ≈2.0). Since Richardson (1948), it is well known that Hale's polarity-law violators happen more often for small (<50 μHem) sunspot groups. The frequency of this violation increases rather steeply with transition to regions of smaller size (Hagenaar, 2001; Tlatov, Vasil'eva, and Pevtsov, 2010; Stenflo and Kosovichev, 2012). Therefore, including smaller and smaller groups into a sample causes increases the anti-Hale region percentage.

The sensitivity of modern instruments (Scherrer *et al.*, 1995, 2012) allows researchers to involve in the statistical studies weaker and weaker ARs. To estimate the magnetic-flux threshold for ARs selection in our study, we evaluated fluxes of several small short-lived ARs from the catalog. We found that the total unsigned magnetic-flux value of short-lived ARs having at least pores of both polarities (according to our criteria) is $\approx 10^{21}$ Mx. This allows us to consider this flux value as an indirect estimate of the threshold for our selection. We presume that counting of ARs with smaller magnetic fluxes is one of the main reasons for the enhanced percentage of anti-Hale groups in recent studies.

Another reason for the discrepancy might be the numerous ambiguities in anti-Hale region identification mentioned in Section 2.2. For example, the detection of anti-Hale ARs in activity complexes is very challenging (Section 2.2, item 2). According to data by Yazev (2011, 2015), there are 321 activity complexes in Solar Cycles 22 – 24, which corresponds 900 – 1100 ARs (9 – 12 % from all ARs). Using average evaluation of anti-Hale ARs percentage ≈4.5 (see the Introduction), we roughly estimate a possible number of anti-Hale regions in activity complexes for three mentioned cycles as 40 – 50 ARs (up to 0.5 % from all ARs). This is an upper limit of anti-Hale ARs number which might be missed in our catalog.

We also compared the anti-Hale regions list for 1989 – 2004 that was used by Sokoloff, Khlystova, and Abramenko (2015) (the 2015 database) with the co-temporal fragment of the compiled catalog. We found that some changes occured in the list of anti-Hale regions; the number of ARs in both databases remains close. The changes turned out to be evenly distributed along the cycle, so that the main inference made by Sokoloff, Khlystova, and Abramenko (2015) about the cycle variations of the relative number of anti-Hale groups did not change.

5. Conclusions

To identify ARs violating the Hale's polarity law, we visually examined sunspot groups from 1 January 1989 to 31 December 2018. This period encompasses the end of the Solar Cycle 22 and the two subsequent cycles including two solar minima, which is important for understanding the coupling between local and global magnetic fields in terms of solar dynamo theory. We used the SOHO/MDI and the SDO/HMI data, as well as the DPD sketches and the MWO catalog and drawings. Detailed comparison of data from different source allowed us to detect a number of ambiguous cases in anti-Hale sunspot groups identification. We analysed the revealed errors and inaccuracies to elaborate the criteria for identification of sunspot groups as anti-Hale ARs. We can conclude the following.

i) The main reasons for possible errors in anti-Hale region identification are:
   a) incorrect determination of AR boundaries;
   b) wrongly distributing of ARs between consecutive cycles during solar minima;
   c) presence of small sunspots/pores with an opposite (to a proper leading polarity by the Hale's law) polarity to the West from the old leading spots in decaying ARs;
   d) emergence of a new magnetic flux within decaying ARs;
   e) the wrong polarity of the most western spots in multipolar ARs;
   f) location of an AR on the Equator;
   g) appearance of the wrong polarity of sunspots located near the limb the projection effect).

ii) Two basic and four additional criteria for identifying bipolar sunspot groups as anti-Hale regions are formulated. Our basic criteria are based on the classical ideas of Hale and Nicholson (1925) and Babcock (1961). Namely, we assume that for an AR to be classified as an anti-Hale region, its dominating features have to form a bipole of reverse polarity with sunspots/pores of both polarities being present. Magnetic connection between the opposite polarities has to be observed.

iii) The catalog of anti-Hale regions for the period of our study is compiled. For each anti-Hale region, the catalog contains: NOAA (or DPD) number; date, coordinates, and corrected total sunspot area at the evolutionary maximum as determined from the DPD and the USAF/NOAA SRS data. The catalog also contains the tilt and Mount Wilson magnetic class. In total, the catalog contains 275 ARs, including 96 small short-lived sunspot groups.

iv) The percentage of sunspot groups violating the Hale's polarity law (meeting the formulated criteria) is ≈3.0 from all studied ARs. This is close to the earliest estimations by the authors who had examined each AR individually: ≈2.4 by Hale and Nicholson (1925) and ≈3.1 by Richardson (1948). Later researchers reported a slightly higher percentage. The enchancement of the percentage might be related to increasing sensitivity of instruments and, therefore, taking into account smaller and smaller bipoles. Another reason for the discrepancy in anti-Hale percentage is the ambiguities in the anti-Hale regions identification mentioned in Section 2.2.

The catalog of anti-Hale regions can be used in studying the phenomena related to the cyclic solar activity. The catalog is available as the Electronic Supplementary Material. The catalog is also available at the CrAO website sun.crao.ru/databases/catalog-anti-hale.

Acknowledgments The authors are thankful to Drs. L.V. Ermakova and A.S. Kutsenko for consulting on complex, ambigous ARs. Efforts of A.V.Zhukova on the catalog compilation were supported by the RSF (Project 18-12-00131). A.I.Khlystova thanks the support of the RFBR's grants 18-02-00085 and 19-52-45002. The work of A.I.Khlystova was supported by the basic financial program of the FSR II.16. D.D.Sokoloff is grateful for the RFBR support under the grant 18-02-00085. V.I.Abramenko would like to acknowledge partial support of the MSHE of RF (Research 0831-2019-0006).

Disclosure of Potential Conflicts of Interest

The authors declare that they have no conflicts of interest.

References

Abramenko, V.I., Zhukova, A.V., Kutsenko, A.S.: 2018, Contributions from Different-Type Active Regions Into the Total Solar Unsigned Magnetic Flux. *Geomag. Aeron.* **58**, 1159. DOI. ADS.

Babcock, H.W.: 1961, The Topology of the Sun's Magnetic Field and the 22-YEAR Cycle. *Astrophys. J.* **133**, 572. DOI. ADS.

Baranyi, T., Győri, L., Ludmány, A.: 2016, On-line Tools for Solar Data Compiled at the Debrecen Observatory and Their Extensions with the Greenwich Sunspot Data. *Solar Phys.* **291**, 3081. DOI. ADS.

Blackman, E.G., Field, G.B.: 2002, New Dynamical Mean-Field Dynamo Theory and Closure Approach. *Phys. Rev. Lett.* **89**, 265007. DOI. ADS.

Brandenburg, A., Subramanian, K.: 2005, Astrophysical magnetic fields and nonlinear dynamo theory. *Phys. Rep.* **417**, 1. DOI. ADS.

Brandenburg, A., Sokoloff, D., Subramanian, K.: 2012, Current Status of Turbulent Dynamo Theory. From Large-Scale to Small-Scale Dynamos. *Space Sci. Rev.* **169**, 123. DOI. ADS.

Hagenaar, H.J.: 2001, Ephemeral Regions on a Sequence of Full-Disk Michelson Doppler Imager Magnetograms. *Astrophys. J.* **555**, 448. DOI. ADS.

Hale, G.E., Nicholson, S.B.: 1925, The Law of Sun-Spot Polarity. *Astrophys. J.* **62**, 270. DOI. ADS.

Hale, G.E., Ellerman, F., Nicholson, S.B., Joy, A.H.: 1919, The Magnetic Polarity of Sun-Spots. *Astrophys. J.* **49**, 153. DOI. ADS.

Hazra, G., Choudhuri, A.R., Miesch, M.S.: 2017, A Theoretical Study of the Build-up of the Sun's Polar Magnetic Field by using a 3D Kinematic Dynamo Model. *Astrophys. J.* **835**, 39. DOI. ADS.

Howard, R.F.: 1989, The Magnetic Fields of Active Regions - Part One. *Solar Phys.* **123**, 271. DOI. ADS.

Jiang, J., Cameron, R.H., Schüssler, M.: 2015, The Cause of the Weak Solar Cycle 24. *Astrophys. J. Lett.* **808**, L28. DOI. ADS.

Kazantsev, A.P.: 1968, Enhancement of a Magnetic Field by a Conducting Fluid. *Sov. J. Exp. Theor. Phys.* **26**, 1031. ADS.

Khlystova, A.I., Sokoloff, D.D.: 2009, Toroidal magnetic field of the Sun from data on Hale-rule-violating sunspot groups. *Astron. Rep.* **53**, 281. DOI. ADS.

Kraichnan, R.H., Nagarajan, S.: 1967, Growth of Turbulent Magnetic Fields. *Phys. Fl.* **10**, 859. DOI. ADS.

Krause, F., Rädler, K.-H.: 1980, *Mean-field magnetohydrodynamics and dynamo theory*. ADS.

Künzel, H.: 1965, Zur Klassifikation von Sonnenfleckengruppen. *Astron. Nachr.* **288**, 177. ADS.

Lefevre, L., Clette, F.: 2014, Survey and Merging of Sunspot Catalogs. *Solar Phys.* **289**, 545. DOI. ADS.

Leighton, R.B.: 1964, Transport of Magnetic Fields on the Sun. *Astrophys. J.* **140**, 1547. DOI. ADS.

Lemen, J.R., Title, A.M., Akin, D.J., Boerner, P.F., Chou, C., Drake, J.F., Duncan, D.W., Edwards, C.G., Friedlaender, F.M., Heyman, G.F., Hurlburt, N.E., Katz, N.L., Kushner, G.D., Levay, M., Lindgren, R.W., Mathur, D.P., McFeaters, E.L., Mitchell, S., Rehse, R.A., Schrijver, C.J., Springer, L.A., Stern, R.A., Tarbell, T.D., Wuelser, J.-P., Wolfson, C.J., Yanari, C., Bookbinder, J.A., Cheimets, P.N., Caldwell, D., Deluca, E.E., Gates, R., Golub, L., Park, S., Podgorski, W.A., Bush, R.I., Scherrer, P.H., Gummin, M.A., Smith, P., Auker, G., Jerram, P., Pool, P., Soufli, R., Windt, D.L., Beardsley, S., Clapp, M., Lang, J., Waltham, N.: 2012, The Atmospheric Imaging Assembly (AIA) on the Solar Dynamics Observatory (SDO). *Solar Phys.* **275**, 17. DOI. ADS.

Li, J.: 2018, A Systematic Study of Hale and Anti-Hale Sunspot Physical Parameters. *Astrophys. J.* **867**, 89. DOI. ADS.

Li, J., Ulrich, R.K.: 2012, Long-term Measurements of Sunspot Magnetic Tilt Angles. *Astrophys. J.* **758**, 115. DOI. ADS.

López Fuentes, M.C., Demoulin, P., Mandrini, C.H., van Driel-Gesztelyi, L.: 2000, The Counterkink Rotation of a Non-Hale Active Region. *Astrophys. J.* **544**, 540. DOI. ADS.

López Fuentes, M.C., Démoulin, P., Mandrini, C.H., Pevtsov, A.A., van Driel-Gesztelyi, L.: 2003, Magnetic twist and writhe of active regions. On the origin of deformed flux tubes. *Astron. Astrophys.* **397**, 305. DOI. ADS.

McClintock, B.H., Norton, A.A., Li, J.: 2014, Re-examining Sunspot Tilt Angle to Include Anti-Hale Statistics. *Astrophys. J.* **797**, 130. DOI. ADS.

Moffatt, H.K.: 1978, *Magnetic Field Generation in Electrically Conducting Fluids*, Cambridge Univ. Press, Cambridge, UK. ADS.

Mordvinov, A.V., Kitchatinov, L.L.: 2019, Evolution of the Sun's Polar Fields and the Poleward Transport of Remnant Magnetic Flux. *Solar Phys.* **294**, 21. DOI. ADS.

Moses, D., Clette, F., Delaboudinière, J.-P., Artzner, G.E., Bougnet, M., Brunaud, J., Carabetian, C., Gabriel, A.H., Hochedez, J.F., Millier, F., Song, X.Y., Au, B., Dere, K.P., Howard, R.A., Kreplin, R., Michels, D.J., Defise, J.M., Jamar, C., Rochus, P., Chauvineau, J.P., Marioge, J.P., Catura, R.C., Lemen, J.R., Shing, L., Stern, R.A., Gurman, J.B., Neupert, W.M., Newmark, J., Thompson, B., Maucherat, A., Portier-Fozzani, F., Berghmans, D., Cugnon, P., van Dessel, E.L., Gabryl, J.R.: 1997, EIT Observations of the Extreme Ultraviolet Sun. *Solar Phys.* **175**, 571. DOI. ADS.

Parker, E.N.: 1955, Hydromagnetic Dynamo Models. *Astrophys. J.* **122**, 293. DOI. ADS.

Rädler, K.-H., Kleeorin, N., Rogachevskii, I.: 2003, The Mean Electromotive Force for MHD Turbulence: The Case of a Weak Mean Magnetic Field and Slow Rotation. *Geophys. Astrophys. Fluid Dyn.* **97**, 249. DOI. ADS.

Richardson, R.S.: 1948, Sunspot Groups of Irregular Magnetic Polarity. *Astrophys. J.* **107**, 78. DOI. ADS.

Ryutova, M.: 2018, Physics of Magnetic Flux Tubes. *Astrophys. Space Sci. Lib.* **455**. DOI. ADS.

Scherrer, P.H., Bogart, R.S., Bush, R.I., Hoeksema, J.T., Kosovichev, A.G., Schou, J., Rosenberg, W., Springer, L., Tarbell, T.D., Title, A., Wolfson, C.J., Zayer, I., MDI Engineering Team: 1995, The Solar Oscillations Investigation - Michelson Doppler Imager. *Solar Phys.* **162**, 129. DOI. ADS.

Scherrer, P.H., Schou, J., Bush, R.I., Kosovichev, A.G., Bogart, R.S., Hoeksema, J.T., Liu, Y., Duvall, T.L., Zhao, J., Title, A.M., Schrijver, C.J., Tarbell, T.D., Tomczyk, S.: 2012, The Helioseismic and Magnetic Imager (HMI) Investigation for the Solar Dynamics Observatory (SDO). *Solar Phys.* **275**, 207. DOI. ADS.

Schunker, H., Baumgartner, C., Birch, A.C., Cameron, R.H., Braun, D.C., Gizon, L.: 2020, Average motion of emerging solar active region polarities. II. Joy's law. *Astron. Astrophys.* **640**, A116. DOI. ADS.

Smith, S.F., Howard, R.: 1968, Magnetic Classification of Active Regions. In: Kiepenheuer, K.O. (ed.) *Structure and Development of Solar Active Regions*, *IAU Symp.* **35**, 33. ADS.

Sokoloff, D., Khlystova, A.I.: 2010, The solar dynamo in the light of the distribution of various sunspot magnetic classes over butterfly diagram. *Astron. Nachr.* **331**, 82. DOI. ADS.

Sokoloff, D., Khlystova, A., Abramenko, V.: 2015, Solar small-scale dynamo and polarity of sunspot groups. *Mon. Not. Roy. Astron. Soc.* **451**, 1522. DOI. ADS.

Stenflo, J.O., Kosovichev, A.G.: 2012, Bipolar Magnetic Regions on the Sun: Global Analysis of the SOHO/MDI Data Set. *Astrophys. J.* **745**, 129. DOI. ADS.

Sur, S., Brandenburg, A., Subramanian, K.: 2008, Kinematic α-effect in isotropic turbulence simulations. *Mon. Not. Roy. Astron. Soc.* **385**, L15. DOI. ADS.

Tlatov, A.G., Vasil'eva, V.V., Pevtsov, A.A.: 2010, Distribution of Magnetic Bipoles on the Sun over Three Solar Cycles. *Astrophys. J.* **717**, 357. DOI. ADS.

van Driel-Gesztelyi, L., Green, L.M.: 2015, Evolution of Active Regions. *Liv. Rev. Solar Phys.* **12**, 1. DOI. ADS.

Vitinsky, Y.I.: 1986, On Sunspot Groups with Irregular Magnetic Polarities. *Byull. Solnechnye Dannye Akad. Nauk SSSR* **9**, 86. ADS.

Wang, Y.-M., Sheeley, J. N. R.: 1989, Average Properties of Bipolar Magnetic Regions during Sunspot CYCLE-21. *Solar Phys.* **124**, 81. DOI. ADS.

Wang, Y.-M., Colaninno, R.C., Baranyi, T., Li, J.: 2015, Active-region Tilt Angles: Magnetic versus White-light Determinations of Joy's Law. *Astrophys. J.* **798**, 50. DOI. ADS.

Yazev, S.A.: 2011, Activity complexes on the sun during the 23rd solar cycle. *Geomag. Aeron.* **51**, 879. DOI. ADS.

Yazev, S.A.: 2015, Activity complexes on the sun in solar cycle 24. *Astron. Rep.* **59**, 228. DOI. ADS.

Zeldovich, Y.B., Ruzmaikin, A.A., Sokoloff, D.D.: 1990, *The Almighty Chance*, World Scientific, Singapore. DOI. ADS.

Zhukova, A.: 2018, A catalog of active regions of the 24th solar cycle. *Izv. Krym. Astrofiz. Obs.* **114**, 74.